

Lattice simulations of QCD-like theories at non-zero density

Jonivar Skullerud

DESY Theory Group, Notkestraße 85, D-22603 Hamburg, Germany

Abstract

One way of avoiding the complex action problem in lattice QCD at non-zero density is to simulate QCD-like theories with a real action, such as two-colour QCD. The symmetries of two-colour QCD with quarks in the fundamental and in the adjoint representation are described, and the status of lattice simulations is reviewed, with particular emphasis on comparison with predictions from chiral perturbation theory. Finally, we discuss how the lessons from two-colour QCD may be carried over to physical QCD.

I. INTRODUCTION

Recently, there has been a considerable interest in QCD at non-zero chemical potential, after a number of model studies have indicated a rich phase structure [1–3] (for a review, see [4]). Clearly, it would be desirable if these predictions could be tested by first-principles, non-perturbative studies, e.g. lattice QCD. Unfortunately, lattice simulations of QCD at non-zero baryon density using standard methods are in practice impossible because the action (and the fermion determinant) becomes complex once the chemical potential is introduced, causing importance sampling to fail. It is possible to split the determinant into a modulus and a phase, simulating with the modulus of the determinant as the measure and reweighting the observables with the phase,

$$\langle O \rangle = \frac{\langle \langle O \arg(\det M) \rangle \rangle}{\langle \langle \arg(\det M) \rangle \rangle}, \quad (1)$$

where $\langle \langle \dots \rangle \rangle$ denotes the expectation value with respect to the positive real measure. However, the denominator in (1) is effectively the ratio of the partition functions of two different theories: the true theory and one with a positive real measure. This should scale as $\exp(-\Delta F)$, where ΔF is the difference in free energy between the two theories. Since the free energy is an extensive quantity, the computational effort required to obtain a reliable sample rises exponentially with the volume.

A number of approaches have been tried to overcome this problem. In the Hamiltonian formalism, the problem does not arise. Analytical results have been obtained in the strong coupling limit [5,6], but so far no method for numerical simulations exists.

With an imaginary chemical potential [7], the action becomes real and positive, so simulations are straightforward. The problem is whether an analytical continuation to real μ is

possible. It works at high temperature [8,9], where also other approaches may be successfully employed [9], but does not seem to be possible at zero or low temperatures. Imaginary chemical potential can also be used to formulate a quenched limit of QCD in the background of a non-zero number of static quarks [10].

Cluster algorithms [11] may provide a way of eliminating the sign problem by summing analytically over configurations in a cluster in such a way that the contribution to the partition function from each cluster is always positive definite. So far, these methods have been applied to a number of spin models; however, an application to QCD has yet to be found.

Finally, the sign problem may be avoided by simulating theories which resemble QCD, but have a real action even at non-zero chemical potential. One such theory is QCD at non-zero isospin density [12,13], which is of intrinsic interest because it corresponds to part of the phase diagram for asymmetric nuclear matter. Another class of theories encompasses two-colour QCD with fermions in the fundamental representation, as well as QCD with adjoint fermions, for any number of colours. The remainder of this review will focus on what can be learnt from lattice simulations of these theories.

II. THEORIES WITH REAL ACTION

The chemical potential μ is introduced on the lattice by multiplying the forward timelike links by e^μ and the backward timelike links by $e^{-\mu}$ [14]. It can be shown [15,16] that the determinant $\det M$ of the fermion matrix M in two-colour QCD is real, even for non-zero μ , both in the continuum and on the lattice. However, it is only possible to demonstrate that it is positive [16] in the cases of continuum or Wilson adjoint fermions and staggered fundamental fermions. Indeed, we will see in section IV that in the case of staggered adjoint fermions there are configurations with a negative determinant, leading to a sign problem at large μ .

A. Symmetry breaking pattern

In the chiral limit, the action for two-colour QCD with N flavours has a $U(N)_L \otimes U(N)_R$ symmetry, which for staggered fermions is manifest as independent $U(N)$ symmetries for the even and odd sites. At $\mu = 0$ this enlarges to a $U(2N)$ symmetry. This can be seen most easily by introducing new fields,

$$\bar{X}_e = (\bar{\chi}_e, -\chi_e^T \tau_2) \quad X_o = \begin{pmatrix} \chi_o \\ -\tau_2 \bar{\chi}_o^T \end{pmatrix} \quad (2)$$

for (staggered) fundamental quarks, and

$$\bar{X}_e = (\bar{\chi}_e, \chi_e^T) \quad X_o = \begin{pmatrix} \chi_o \\ \bar{\chi}_o^T \end{pmatrix} \quad (3)$$

for adjoint quarks. The action can then be written as

$$S = \frac{1}{2} \sum_{x_e, \nu} \eta_\nu(x) \left[\bar{X}_e(x) \begin{pmatrix} e^{\mu\delta_{\nu,0}} & 0 \\ 0 & e^{-\mu\delta_{\nu,0}} \end{pmatrix} U_\nu(x) X_o(x + \hat{\nu}) - \right. \\ \left. \bar{X}_e(x) \begin{pmatrix} e^{-\mu\delta_{\nu,0}} & 0 \\ 0 & e^{\mu\delta_{\nu,0}} \end{pmatrix} U_\nu^\dagger(x - \hat{\nu}) X_o(x - \hat{\nu}) \right] \quad (4)$$

where x_e denotes the even sites. In the continuum, the equivalent fields are

$$\text{fundamental: } \Psi = \begin{pmatrix} \psi_L \\ \sigma_2 \tau_2 \psi_R^* \end{pmatrix} \quad \text{adjoint: } \Psi = \begin{pmatrix} \psi_L \\ \sigma_2 \psi_R^* \end{pmatrix} \quad (5)$$

which gives the continuum lagrangian

$$\mathcal{L} = i\Psi^\dagger \sigma_\nu (D_\nu - \mu B_\nu) \Psi \quad B_\nu = \begin{pmatrix} 1 & 0 \\ 0 & -1 \end{pmatrix} \delta_{\nu 0}. \quad (6)$$

The explicit chiral symmetry breaking term in the Wilson fermion action means that there is no equivalent enlarged symmetry for Wilson fermions; however, new fields may be introduced analogously to the continuum case, and the enlarged symmetries will be broken by $\mathcal{O}(a)$ terms in the action.

The chiral condensate can be written in terms of the new fields,

$$\bar{\chi}\chi = \bar{X}_e \begin{pmatrix} 0 & \mathbb{1} \\ \pm \mathbb{1} & 0 \end{pmatrix} \frac{T}{2} \bar{X}_e^{tr} + X_o^{tr} \begin{pmatrix} 0 & \mathbb{1} \\ \pm \mathbb{1} & 0 \end{pmatrix} \frac{T}{2} X_o \quad (7)$$

for staggered fermions, and

$$\bar{\psi}\psi = \Psi^T \sigma_2 \frac{T}{2} \begin{pmatrix} 0 & -\mathbb{1} \\ \pm \mathbb{1} & 0 \end{pmatrix} \Psi + \text{h.c.} \quad (8)$$

in the continuum and for Wilson fermions. In both cases, the $+$ sign is for fundamental fermions and the $-$ sign for adjoint, while T is τ_2 for fundamental fermions and 1 for adjoint. A nonzero chiral condensate thereby breaks down the $U(2N)$ symmetry to $O(2N)$ for fundamental fermions and $Sp(2N)$ for adjoint fermions, giving rise to $N(2N + 1)$ and $N(2N - 1)$ Goldstone modes respectively. Of these, there will be N^2 mesonic states, while the remaining $N(N \pm 1)$ will be diquarks. In the continuum, and for Wilson fermions, the pattern will be the opposite (modulo the 1 mode destroyed by the axial anomaly in the continuum), but for 1 flavour of fundamental quarks, there is no chiral symmetry in the first place. From this we see that in the case of $N = 1$ adjoint staggered fermions, and only in this case, are there no diquark Goldstone modes.

For $m \neq 0$, all the pseudo-Goldstone modes remain degenerate, with masses $m_\pi \propto \sqrt{m}$. As the chemical potential μ increases, the ground state will begin to be populated with baryonic matter. The transition to a ground state containing matter occurs when $\mu = \mu_o \simeq m_b/n_q$, where m_b is the mass of the lightest baryon, and this baryon contains n_q quarks. At this point, the baryon number density n becomes non-zero, where n is given by

$$n = \frac{1}{2} \langle \bar{\psi}(x) e^\mu (\gamma_0 - 1) U_0(x) \psi(x + \hat{0}) + \bar{\psi}(x + \hat{0}) e^{-\mu} (\gamma_0 + 1) U_0^\dagger(x) \psi(x) \rangle \quad (9)$$

for Wilson fermions, and

$$n = \frac{1}{2} \langle \bar{\chi}(x) \eta_0(x) [e^\mu U_0(x) \chi(x + \hat{0}) + e^{-\mu} U_0^\dagger(x - \hat{0}) \chi(x - \hat{0})] \rangle. \quad (10)$$

for staggered fermions. Where there are diquark Goldstone modes, those states will be the lightest baryons in the spectrum. This means that for most variants of two-colour QCD we expect $\mu_o \simeq m_\pi/2$, in contrast to the much larger value $m_N/3$ expected in real (three-colour) QCD. The exception is two-colour QCD with one flavour of adjoint staggered quarks.

In the limit of small m and μ , the behaviour of $\langle \bar{\psi}\psi \rangle$, the diquark condensate $\langle \psi\psi \rangle$, and n as functions of m and μ can be calculated in chiral perturbation theory. If we define the rescaled variables

$$x = \frac{2\mu}{m_{\pi 0}}, \quad y = \frac{\langle \bar{\psi}\psi \rangle}{\langle \bar{\psi}\psi \rangle_0}, \quad z = \frac{\langle \psi\psi \rangle}{\langle \psi\psi \rangle_0}, \quad \tilde{n} = \frac{m_{\pi 0} n}{8m \langle \psi\psi \rangle_0}, \quad (11)$$

where the 0 subscript denotes values at $\mu = 0$, the prediction from χ PT for the models with diquark Goldstone modes is [15]

$$y = \begin{cases} 1 \\ \frac{1}{x^2} \end{cases} \quad z = \begin{cases} 0 \\ \sqrt{1 - \frac{1}{x^4}} \end{cases} \quad \tilde{n} = \begin{cases} 0 \\ \frac{x}{4} \left(1 - \frac{1}{x^4}\right) \end{cases} \quad ; x < 1 \\ ; x > 1 \end{cases} \quad (12)$$

B. Diquark condensation

At large chemical potential, the relevant degrees of freedom will be quarks with momenta near the Fermi surface. The attractive quark–quark interaction will give rise to instability with respect to condensation of diquark pairs at opposite sides of the Fermi surface. In physical QCD, the diquark condensate cannot be a colour singlet, so the gauge symmetry is spontaneously broken, giving rise to the phenomenon of colour superconductivity.

In two-colour QCD, on the other hand, there may be the possibility of gauge singlet diquarks, which will be energetically favoured compared to non-singlet states. Indeed, in the previous section we saw that most variants of two-colour QCD have diquark Goldstone modes, which will be the preferred channel for diquark condensation. In the $N = 1$ staggered adjoint model, this is not the case, and we do not know *a priori* in which channel the condensation will occur. We must proceed by constructing possible operators which obey the Pauli principle and making additional assumptions about locality, Lorentz structure and gauge invariance [16]. At least one of the possible condensates constructed this way gives rise to a colour superconducting ground state.

The standard way of computing the diquark condensate on the lattice is to introduce a diquark source term into the action [17]. For two-colour QCD with fundamental staggered quarks the action then becomes

$$S_F = \sum_{x,y} \bar{\chi}(x) M_{xy} \chi(y) + \sum_x \frac{j}{2} \left[\chi^T(x) \tau_2 \chi(x) + \bar{\chi}(x) \tau_2 \bar{\chi}^T(x) \right] \quad (13)$$

$$= (\bar{\chi}, \chi^T) \begin{pmatrix} j\tau_2 & \frac{1}{2}M \\ \frac{1}{2}M & j\tau_2 \end{pmatrix} \begin{pmatrix} \bar{\chi}^T \\ \chi \end{pmatrix} \equiv X^T \mathcal{A}[j] X. \quad (14)$$

In this case, the partition function becomes proportional to the Pfaffian $\text{Pf}\mathcal{A}[j]$. The diquark condensate $\langle\chi^T\tau_2\chi\rangle$ may be evaluated by taking

$$\langle\chi^T\tau_2\chi\rangle = \lim_{j\rightarrow 0} \frac{1}{2V} \left\langle \text{Tr} \left\{ \mathcal{A}^{-1} \begin{pmatrix} \tau_2 & 0 \\ 0 & \tau_2 \end{pmatrix} \right\} \right\rangle \quad (15)$$

An alternative approach [18] is to rewrite the Pfaffian as

$$\text{Pf}\mathcal{A}[j] = \text{Pf}(B + j) = \pm \sqrt{\det(B + j)} \quad (16)$$

where

$$B = \begin{pmatrix} 0 & \frac{1}{2}M\tau_2 \\ -\frac{1}{2}M\tau_2 & 0 \end{pmatrix}. \quad (17)$$

This can be expanded as a polynomial in j by diagonalising B^2 , obviating the need to simulate at non-zero diquark source. Since this gives the Pfaffian at any j , it can also be used to determine the diquark condensate using the probability distribution function [19].

III. SIMULATIONS WITH FUNDAMENTAL QUARKS

In the past year and a half, a number of groups have been performing lattice simulations of two-colour QCD with fundamental staggered fermions both at zero [20–23,13] and non-zero [24,25] temperature. Also, one group is performing simulations with Wilson fermions [26].

Aloisio *et al.* [21,22] have performed simulations in the strong coupling limit for a number of quark masses, flavours and lattice volumes. Fig. 1 shows results for the chiral condensate, the diquark condensate and the baryon number density, at $m = 0.2$ and a non-zero source $j = 0.02$, for two different lattice sizes. Also shown are the χ PT predictions from (12). The agreement between the prediction and the numerical results is quite striking, considering that this is far from the continuum limit. This suggests a weak β dependence. Fig. 2 shows the diquark condensate at zero diquark source, for $N_f = 1$ and a range of quark masses. Again, we see a very good agreement with the prediction (12). At larger μ , we see that the value of $\langle\psi\psi\rangle$ drops, going to zero at high μ . This second transition is due to lattice artefacts connected with the saturation of lattice sites with fermions. In the infinite volume limit it is expected to disappear.

Simulations at non-zero μ with a diquark source have been performed by Kogut and Sinclair [13]. Results for the diquark condensate and chiral condensate are shown in fig. 3. Again, we see the chiral condensate dropping and the diquark condensate rising for $\mu \gtrsim m_\pi/2$, in agreement with χ PT. We also see the same large- μ saturation behaviour for the diquark condensate as in [22]. Fig. 4 shows results for pion and scalar diquark masses. The scalar diquark mass falls roughly as $m_\pi - 2\mu$ as μ approaches $m_\pi/2$. The pion mass remains constant up to $\mu \approx m_\pi/2$, after which it falls to zero. This is again in accordance with the expectation from χ PT.

The spectrum of the Dirac operator has been studied in some detail by the Vienna group [23] for staggered fermions and by the Hiroshima group [26] for Wilson fermions. A preliminary study of topology at non-zero temperature has also been performed [24].

IV. SIMULATIONS WITH ADJOINT QUARKS

As indicated in section II A, two-colour QCD with one flavour of adjoint staggered fermions has features which makes it in some senses more ‘QCD-like’ than other variants of two-colour QCD. In particular, it has no diquark Goldstone modes, so we expect an onset transition at a value of the chemical potential different from $m_\pi/2$ — possibly at $\mu = m_N/3$ where m_N denotes the mass of the lightest three-quark baryon (the ‘nucleon’). It also has a sign problem.

The theory has been simulated [16,27] using two different algorithms: Hybrid Monte Carlo, which is not able to change the sign of the determinant, and therefore only simulates the positive determinant sector of the theory, and the two-step multibosonic algorithm [28], which is able to take the sign properly into account. Figs 5 and 6 show the results from HMC simulations for y and \tilde{n} of (11) respectively, for a range of values for the quark mass m and chemical potential μ . Up to $x \sim 1.5$, the data collapse onto a universal curve, which agrees well with the predictions of (12). Even at larger x , the data for the chiral condensate lie close to the χ PT prediction. At $x \gtrsim 2$, however, the data for different m diverge, indicating that χ PT may be breaking down. Results for the plaquette [27] show a drop in its value for $\mu \geq m_\pi/2$, presumably due to Pauli blocking, while the pion mass appears to agree with the χ PT prediction $m_\pi = 2\mu$ at $x > 2$.

The agreement between the predictions of χ PT and these results paradoxically enough presents a problem, since this model is not supposed to contain any diquark Goldstone modes, and thus the χ PT predictions of (12) are not valid in this case. In particular, there should not be any onset transition at $\mu = m_\pi/2$. The suspicion must be that this contradiction is due to the fact that HMC does not change the sign of the determinant, and that it therefore simulates the wrong theory — a theory with conjugate quarks.

The simulation points for the TSMB algorithm were selected to focus on the effect of the sign, with one point at $\mu = 0$, one just past the HMC onset transition, and one deeper into the dense region. With this algorithm, a reweighting factor r and the sign of $\det M$ must be determined for each configuration [29]. The expectation value of an observable O is then determined by the ratio

$$\langle O \rangle = \frac{\langle O \times r \times \text{sign} \rangle}{\langle r \times \text{sign} \rangle}. \quad (18)$$

The results for $\langle \bar{\psi}\psi \rangle$ and n , together with the corresponding HMC results, are summarised in Table I. For TSMB at $\mu \neq 0$ we also include observables determined separately in each sign sector, defined by $\langle O \rangle_\pm = \langle O \times r \rangle_\pm / \langle r \rangle_\pm$. At $\mu = 0.0$ the two algorithms agree, as they should. Also, the results in the positive determinant sector for TSMB at larger μ agree with the HMC results. However, the results for the negative determinant sector are significantly different. This difference has the effect of bringing the average both for $\langle \bar{\psi}\psi \rangle$ and for n back to values consistent with the $\mu = 0$ values. This is an indication that at $\mu = 0.36$ and quite possibly also at $\mu = 0.4$, the system is still in the vacuum phase, which means that the onset transition in this model occurs at a larger μ than for other variants of two-colour QCD. This is consistent with the symmetry-based arguments of section II A that this model has no baryonic Goldstone modes.

V. CONCLUSIONS

Substantial progress has been made recently in lattice simulations of two-colour QCD at non-zero density, with both fundamental and adjoint quarks. The simulations with fundamental quarks nicely reproduce the predictions from chiral perturbation theory for the chiral condensate, diquark condensate, and baryon density, except at very large chemical potentials. Here, saturation effects are observed, especially for the diquark condensate. The meson and diquark spectrum is also being analysed, with preliminary results for the pion and scalar diquark masses again in rough agreement with chiral perturbation theory.

Two-colour QCD with one flavour of adjoint staggered quark is not expected to have any diquark Goldstone modes, unlike all other variants of two-colour QCD. It also has a sign problem. Simulations of this model restricted to the sector with a positive fermion determinant reproduce the predictions of chiral perturbation theory for theories with diquark Goldstone modes, including an early onset transition at $\mu \approx m_\pi/2$ — although the breakdown of χ PT may be observed at larger μ . When configurations with negative determinants are included, we find a strong correlation between the sign and the value of observables. This effect appears to lead to a cancellation of the early onset transition. This observation may hold the key to understanding the problem of the premature onset which has bedevilled previous attempts to simulate physical QCD at non-zero density.

The presence of diquark modes which are degenerate with the pion means that the study two-colour QCD is of limited usefulness when it comes to studying directly the onset transition, hadron spectrum and diquark condensation in physical QCD at non-zero density. However, useful experience may be gained by comparing the results of lattice simulations with those of other methods which are also applicable to physical QCD. Of particular interest would be the study of gluodynamics, where SU(2) and SU(3) are expected to exhibit similar behaviour, even at non-zero μ . Thus it might be possible to cast light on the deconfinement transition at high μ and low T by studying two-colour QCD.

ACKNOWLEDGEMENTS

This work is supported by the TMR network “Finite temperature phase transitions in particle physics”, EU contract ERBFMRX-CT97-0122.

REFERENCES

- [1] M. Alford, K. Rajagopal, and F. Wilczek, Nucl. Phys. **B537**, 443 (1999), hep-ph/9804403.
- [2] M. Alford, K. Rajagopal, and F. Wilczek, Phys. Lett. **B422**, 247 (1998), hep-ph/9711395.
- [3] R. Rapp, T. Schäfer, E. V. Shuryak, and M. Velkovsky, Phys. Rev. Lett. **81**, 53 (1998), hep-ph/9711396.
- [4] K. Rajagopal and F. Wilczek, (2000), hep-ph/0011333.
- [5] E. B. Gregory, S.-H. Guo, H. Kröger, and X.-Q. Luo, Phys. Rev. **D62**, 054508 (2000), hep-lat/9912054.
- [6] X.-Q. Luo, E. B. Gregory, S.-H. Guo, and H. Kröger, (2000), hep-ph/0011120.
- [7] M. Alford, A. Kapustin, and F. Wilczek, Phys. Rev. **D59**, 054502 (1999), hep-lat/9807039.
- [8] M.-P. Lombardo, Nucl. Phys. Proc. Suppl. **83**, 375 (2000), hep-lat/9908006.
- [9] A. Hart, M. Laine, and O. Philipsen, (2000), hep-lat/0010008.
- [10] J. Engels, O. Kaczmarek, F. Karsch, and E. Laermann, Nucl. Phys. **B558**, 307 (1999), hep-lat/9903030.
- [11] S. Chandrasekharan, (2000), hep-lat/0011022.
- [12] D. T. Son and M. A. Stephanov, (2000), hep-ph/0005225.
- [13] S. J. Hands, J. B. Kogut, S. E. Morrison, and D. K. Sinclair, (2000), hep-lat/0010028.
- [14] P. Hasenfratz and F. Karsch, Phys. Lett. **B125**, 308 (1983).
- [15] J. B. Kogut, M. A. Stephanov, D. Toublan, J. J. M. Verbaarschot, and A. Zhitnitsky, Nucl. Phys. **B582**, 477 (2000), hep-ph/0001171.
- [16] S. Hands *et al.*, Eur. Phys. J. **C17**, 285 (2000), hep-lat/0006018.
- [17] S. Morrison and S. Hands, Two colours qcd at nonzero chemical potential, in *Strong and Electroweak Matter, Copenhagen, 1998*, p. 364, 1999, hep-lat/9902012.
- [18] R. Aloisio, A. Galante, V. Azcoiti, G. D. Carlo, and A. F. Grillo, (2000), hep-lat/0007018.
- [19] V. Azcoiti, V. Laliena, and X.-Q. Luo, Phys. Lett. **B354**, 111 (1995), hep-th/9509091.
- [20] S. Hands and S. Morrison, Diquark condensation in dense matter: A lattice perspective, in *Understanding Deconfinement in QCD*, edited by D. Blaschke *et al.*, p. 31, Singapore, 2000, World Scientific, hep-lat/9905021.
- [21] R. Aloisio, V. Azcoiti, G. D. Carlo, A. Galante, and A. F. Grillo, (2000), hep-lat/0009034.
- [22] R. Aloisio, V. Azcoiti, G. D. Carlo, A. Galante, and A. F. Grillo, (2000), hep-lat/0011079.
- [23] E. Bittner, M.-P. Lombardo, H. Markum, and R. Pullirsch, (2000), hep-lat/0010018.
- [24] B. Alles, M. D’Elia, M. P. Lombardo, and M. Pepe, (2000), hep-lat/0010068.
- [25] Y. Liu, O. Miyamura, A. Nakamura, and T. Takaishi, (2000), hep-lat/0009009.
- [26] S. Muroya, A. Nakamura, and C. Nonaka, (2000), hep-lat/0010073.
- [27] S. Hands, I. Montvay, M. Oevers, L. Scorzato, and J. Skullerud, (2000), hep-lat/0010085.
- [28] I. Montvay, Nucl. Phys. **B466**, 259 (1996), hep-lat/9510042.
- [29] I. Montvay, (1999), hep-lat/9903029.

FIGURES

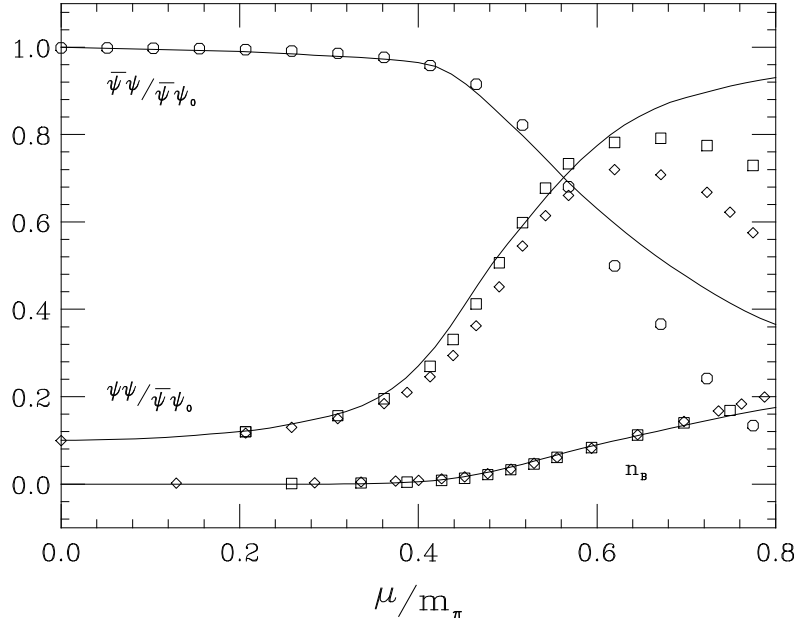


FIG. 1. Baryon density, chiral condensate and diquark condensate vs. chemical potential, from [21]. The solid lines are the predictions of (12).

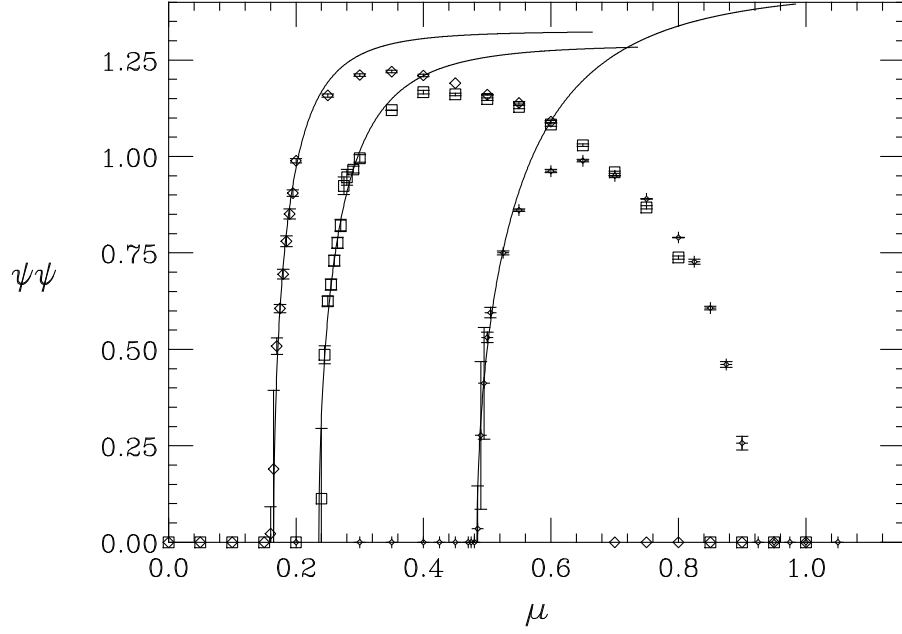


FIG. 2. Diquark condensate for a 6^4 lattice, $N_f = 1$, for $m = 0.025$ (diamonds), 0.05 (squares) and 0.2 (stars) at strong coupling, from [22], with the predictions of (12).

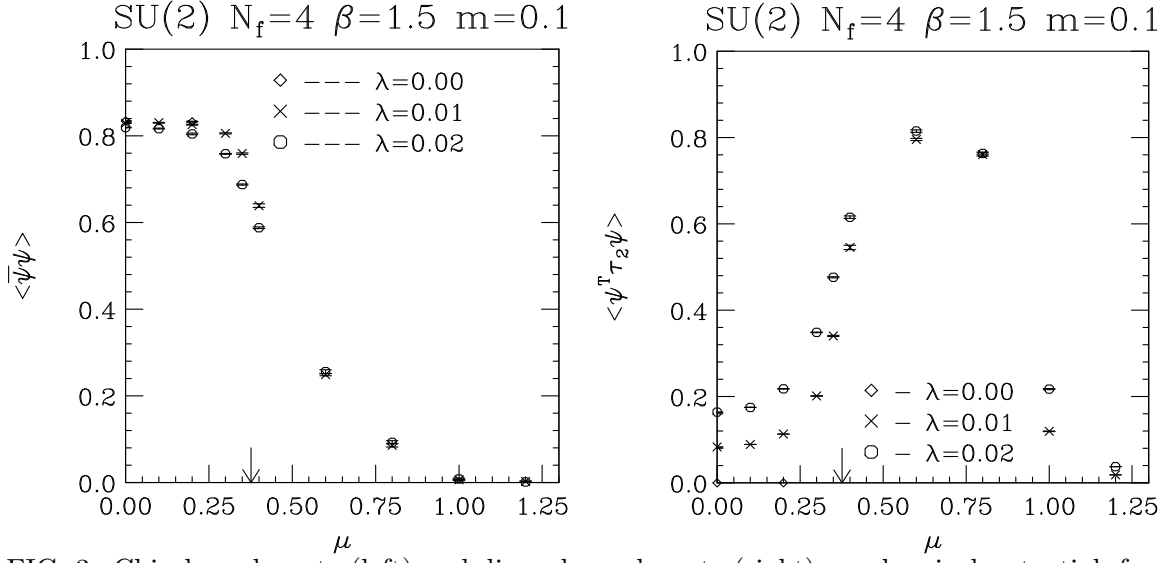


FIG. 3. Chiral condensate (left) and diquark condensate (right) vs. chemical potential, for one flavour fundamental staggered quarks, on an 8^4 lattice; from [13]. The arrow indicates $\mu \approx m_\pi/2$.

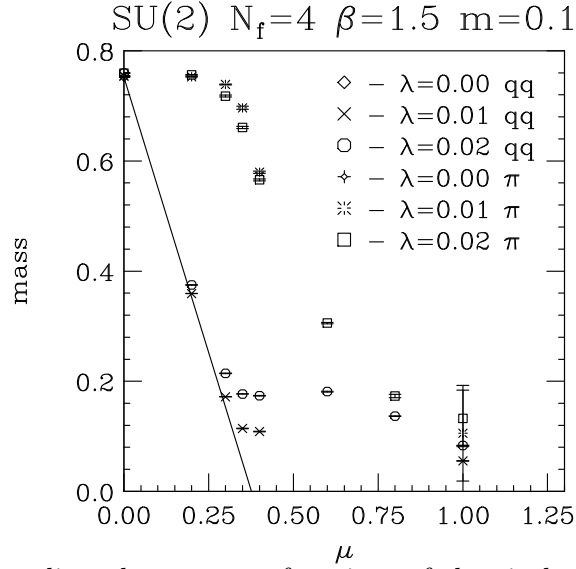


FIG. 4. Pion and scalar diquark masses as functions of chemical potential, for one flavour of fundamental staggered quarks, on an 8^4 lattice; from [13]. The straight line is $m = m_\pi - 2\mu$.

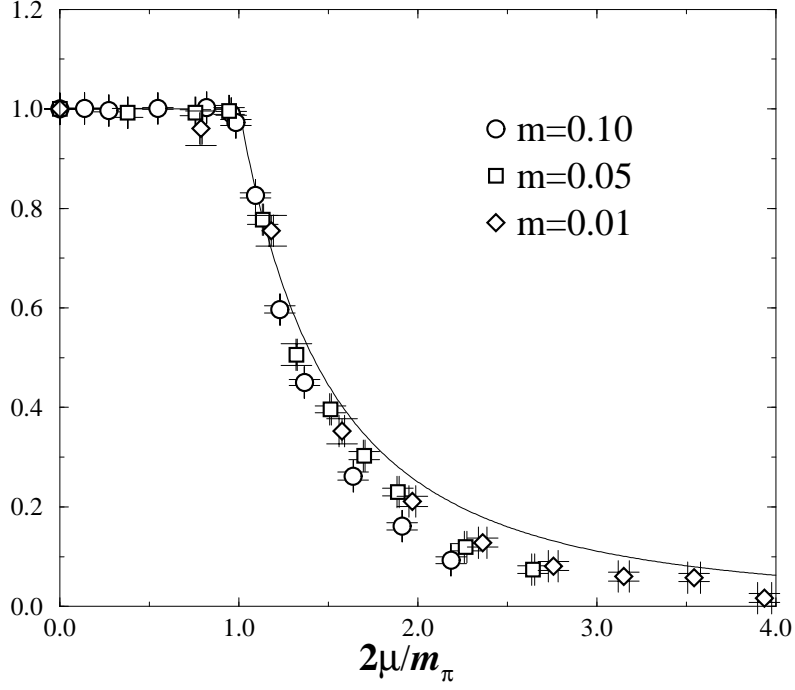


FIG. 5. Chiral condensate vs. chemical potential for one flavour of adjoint staggered quarks, using the rescaled variables of eq. (11); from [27].

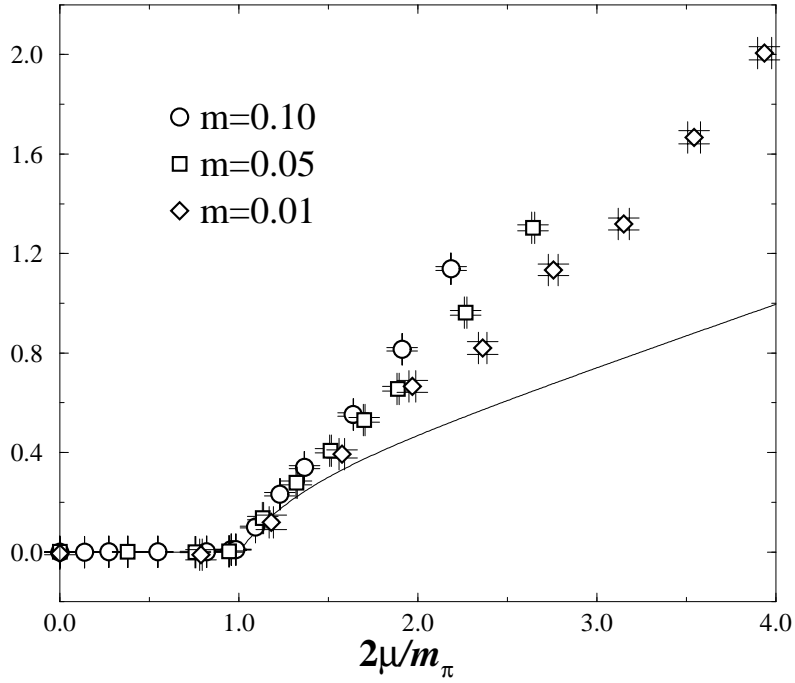


FIG. 6. Baryon density vs. chemical potential for one flavour of adjoint staggered quarks, using the rescaled variables of eq. (11); from [27].

TABLES

	μ	TSMB			HMC
		$\langle O \rangle$	$\langle O \rangle_+$	$\langle O \rangle_-$	
$\langle \bar{\chi} \chi \rangle$	0.0	1.525(3)			1.526(1)
	0.36	1.551(10)	1.521(8)	1.176(37)	1.485(9)
	0.4	1.50(15)	1.248(17)	1.177(20)	1.253(10)
n	0.0	0.0000(13)			-0.0002(3)
	0.36	-0.0003(80)	0.0199(64)	0.252(32)	0.0172(28)
	0.4	0.07(10)	0.177(14)	0.208(15)	0.1667(90)

TABLE I. A comparison of results between TSMB and HMC for one flavour of adjoint staggered quarks. Due to long autocorrelation times, the errors in the HMC results are probably underestimated.